plant biology

Micromorphological and phytochemical survey on Ballota acetabulosa (L.) Benth.

Journal:	*Plant Biology*
Manuscript ID	Draft
Manuscript Type:	Research Paper
Date Submitted by the Author:	n/a
Complete List of Authors:	Giuliani, Claudia; University of Milan , Pharmaceutical Sciences Bottoni, Martina; University of Milan, Department of Pharmaceutical Sciences Ascrizzi, Roberta Milani, Fabrizia; Università degli Studi di Milano Falsini, Sara; Università degli Studi di Firenze Papini, Alessio Flamini, Guido Fico, Gelsomina; University of Milan , Pharmaceutical Sciences
Keyword:	Greek horehound, Lamiaceae, Microscopy, HS-SPME, trichome morphotypes, VOCs profile

Micromorphological and phytochemical survey on *Ballota acetabulosa* (L.) Benth.

Claudia Giuliani [a,b], Martina Bottoni [a,b], Roberta Ascrizzi [c], Fabrizia Milani [a,b], Sara Falsini [e], Alessio Papini [e], Guido Flamini [c], Gelsomina Fico [a,b]

[a] Department of Pharmaceutical Sciences, University of Milan, Via Mangiagalli 25, I-20133 Milan, Italy

[b] Ghirardi Botanic Garden, Department of Pharmaceutical Sciences, University of Milan, Via Religione 25, I-25088 Toscolano Maderno, Brescia, Italy

[c] Department of Pharmacy, University of Pisa, Via Bonanno 6, I-56126 Pisa, Italy

[d] Department of Chemistry, University of Milan, Via Golgi 19, I-20133 Milan, Italy

[e] Department of Biology, University of Florence, Via La Pira 4, I-50121 Florence, Italy

Running head

Ballota acetabulosa: trichomes and volatiles.

Corresponding author

Dr. Martina Bottoni
Department of Pharmaceutical Sciences, University of Milan, Via Mangiagalli 25, 20133 Milan, Italy; martina.bottoni@unimi.it

Keywords

Greek horehound, Lamiaceae, Microscopy, HS-SPME, trichome morphotypes, VOCs profile.

One-sentence summary

Micromorphological and phytochemical surveys were performed on *Ballota acetabulosa* (L.) Benth. revealing two elements of novelty: histochemistry and VOC characterization.

Abstract

- Within the Open Science project entitled "Botanic Garden, factory of molecules", a multidisciplinary study approach was applied on *Ballota acetabulosa* (L.) Benth., preserved at the Ghirardi Botanic Garden (Toscolano Maderno, BS, Italy).

- Micromorphological, histochemical, and phytochemical investigations were conducted on the vegetative and reproductive organs. For the first time, this survey reported the histochemical assays and the ultrastructural observations on the secreting structures, as well as the characterization of the volatiles spontaneously emitted from leaves and flowers.

- Four trichome morphotypes were identified: peltate and short-stalked, medium-stalked, and long-stalked capitate trichomes, each with a peculiar distribution pattern. The histochemical analysis was confirmed by the ultrastructural observations, with the peltates and long-stalked capitates as the main sites responsible for terpene production. The head-space characterization revealed that sesquiterpene hydrocarbons prevailed both in leaves and flowers, with γ-muurolene, β-caryophyllene, and (*E*)-nerolidol as the most abundant compounds. Moreover, a comparison with literature data concerning the ecological roles of the main compounds suggested a dominant defensive action both at the leaf and flower level.

- Therefore, we correlated the trichome morphotypes with the production of secondary metabolites, in the attempt to link these data to their potential ecological meanings. Finally, we made the obtained scientific knowledge available to the visitors of the Botanic Garden through the realization of a new labelling dedicated to *B. acetabulosa* that highlights the "invisible", microscopic features of the plant.

Introduction

The genus *Ballota* L. (Lamiaceae) includes about 35 perennial herbs and subshrubs, native to the temperate regions of Asia, Africa and Europe, with its largest centre of diversity located in the Mediterranean Basin (Morteza-Semnani & Ghanbarimasir 2019). The traditional medicine ascribes to them antiemetic, antispasmodic, sedative, vermifuge, and antitussive properties (Yazgan *et al.* 2010; Morteza-Semnani & Ghanbarimasir 2019).

Ballota acetabulosa (L.) Benth., known as Greek horehound, is a perennial herb native to Greece and the Aegean region, reaching up to 60-80 cm in height, woody at the base, with greyish-tomentose stems covered by simple and stellate hairs; middle and upper cauline leaves, crenate-dentate, with a petiole 5-15 mm long; bracteoles linear to spathulate, membranous; the inflorescences are verticillasters, 6-12 flowered; the calyx is 12-15 mm long and the corolla is 15-18 mm long, purple and white in colour (Tutin *et al.* 1972).

In the traditional Greek and Roman medicines, *B. acetabulosa* was an ingredient of the *Dictamnus*, the common name of a complex of medicinal species belonging to the Rutaceae and Lamiaceae families, useful in the treatment of gynaecological disorders and affections of different origins (Martínez-Francés *et al.* 2015).

Regarding the morphological and phytochemical characterization of the species, the available contributions are few. In this regard, the micromorphological literature proposes two dated investigations focused on leaves (Psaras 1986; Psaras & Rhizopoulou 1995) and one study concerning the anatomy of the aerial vegetative organs, in which references to glandular and non-glandular trichomes are reported (Yazgan *et al.* 2010).

In the phytochemical field, there are no studies focused on the profile of the volatile organic compounds (VOCs), while several works on the essential oil composition of congeneric species exist, often linked to evaluations of their biological activity (Morteza-Semnani & Ghanbarimasir 2019; Rosselli *et al.* 2019). Among the most recent works, for example, investigations on *B. bullata*, *B. nigra* subsp. *uncinata* and subsp. *foetida*, *B. undulata*, *B. saxatilis*, and *B. hispanica* are counted, some of which referring to Italian samples (Riccobono *et al.* 2016; Rigano *et al.* 2017, 2020; El Mokni *et al.* 2020). As for *B. acetabulosa*, several studies about the characterization of extracts with increasing polarity (petroleum ether, ethyl acetate, methanol),

ethanol, methanol and aqueous ones, related to their potential biological activity (antifungal, antimicrobial, antioxidant, cytotoxic) exist, as well as analysis on the composition of the polyphenolic, flavonoidic, and diterpenic content (Sahpaz *et al.* 2002; Couladis *et al.* 2003; Yilmaz & Çitoğlu 2003; Dumlu & Bulut 2007; Dulger & Kilcik 2011a, 2011b; Dulger & Dulger 2012; Askun *et al.* 2013; Rosselli *et al.* 2019).

In this context, this work aims to increase knowledge on *B. acetabulosa* in the micromorphological and phytochemical fields through complementary investigation approaches. The primary goals are: **1.** the description of the morphology and the distribution pattern of non-glandular and glandular trichomes by means of Light Microscopy and Scanning Electron Microscopy; **2.** the analysis, reported here for the first time, of the main compound classes secreted by glandular trichomes through histochemical assays; **3.** the study of the ultrastructural features of the secreting cells by means of Transmission Electron Microscopy, in order to identify the cellular compartments involved in the secretory process; **4.** the characterization, as element of novelty, of the VOCs spontaneously emitted by leaves and flowers, and **5.** the correlation of the VOC profiles with the potential ecological role through the analysis of the literature data concerning the ecological action of the dominant compounds.

Finally, the present work is part of a wider project entitled "Botanic Garden, factory of molecules", aimed at investigating a selection of species preserved at the Ghirardi Botanic Garden (Toscolano Maderno, BS, Italy) through a multi-level study approach: micromorphological, phytochemical, and concerning the ecology and the biological activity of the secondary metabolites. The achieved results converged in the realization of a new iconographic apparatus dedicated to *B. acetabulosa*, showing the results of the scientific research to the general public.

Materials and methods

Plant material

Ballota acetabulosa is preserved at the Ghirardi Botanic Garden (Toscolano Maderno, BS, Lombardy, Italy) of the Department of Pharmaceutical Sciences of the University of Milan.

Samplings for the micromorphological and phytochemical investigations were performed in June 2019. Voucher specimens were labelled with the code GBG2019/027 and deposited in the *Herbarium* of the Ghirardi Botanic Garden.

Micromorphology

The micromorphology, localization and histochemistry, together with the ultrastructural features of trichomes on the vegetative and reproductive organs were studied by means of Light Microscopy (LM), Scanning Electron Microscopy (SEM) and Transmission Electron Microscopy (TEM).

We examined at least ten replicates per each plant part to evaluate the variability of the micromorphological features. Referring to the trichomes localization on the examined plant parts, we qualitatively evaluated their distribution using the following symbols: (-) missing, not observed in any of the replicates; (±) sporadic in no more than four replicates; (+) present in all replicates; (++) abundant in all replicates, with a distribution on the whole organ surface.

Light microscopy (LM) - Fresh and FAA-fixed samples were analysed. The fresh material was hand-sectioned, while the fixed samples were dehydrated in ascending ethanol series up to absolute, embedded in Technovit/Historesin and sectioned with a microtome. The following histochemical stainings were employed: Toluidine Blue as a general dye (Beccari & Mazzi 1966), Fluoral Yellow-088 for total lipids (Brundrett *et al.* 1991), Nile Red for neutral lipids (Greenspan *et al.* 1985), Nadi reagent for terpenes (David *et al.* 1964), Ruthenium Red for acid polysaccharides (Jensen 1962), Alcian Blue for mucopolysaccharides (Beccari & Mazzi 1966), and Ferric Trichloride for polyphenols (Gahan 1984). Control procedures were concurrently performed. Observations were made with a Leitz DM-RB Fluo optical microscope equipped with a Nikon digital camera.

Scanning Electron Microscopy (SEM) - Small segments of leaves, sepals and petals and floral pedicels were fixed in FAA solution (formaldehyde:acetic acid:ethanol 70% = 5:5:90) for 10 days, dehydrated in an ascending ethanol series up to absolute and critical point-dried. The samples were mounted on aluminium stubs, gold-coated and observed under a Philips XL 20 SEM operating at 10 kV.

Transmission Electron Microscopy (TEM) - Small pieces of plant material were fixed in 2.5% glutaraldehyde in 0.1 M phosphate buffer at pH 6.8 and post fixed in 2% OsO4 in the same phosphate buffer, dehydrated and embedded in Spurr's resin. Ultrathin sections were stained with uranyl acetate and lead citrate. The samples were observed under a Philips EM-300 TEM.

Phytochemistry

Volatile Organic Compounds (VOCs)

Three leaves and three flowers were cut and immediately inserted into separate glass vials of suitable volume for the analysis.

HS-SPME Sample analysis – The headspace sampling conditions were as reported in Ascrizzi et al., 2017 (Ascrizzi *et al.* 2017). For the headspace samplings, Supelco SPME (Solid Phase Micro-Extraction) devices, coated with polydimethylsiloxane (PDMS, 100 µm) were used; the same new fibre, preconditioned according to the manufacturer instructions, was employed for all analyses. To ensure a stable temperature, samplings were conducted in an air-conditioned room at 22 ± 1°C; this temperature was chosen to avoid the thermal damage of the plant material and, thus, any artificial-induced volatiles release. After 30 min of equilibration, the fibre was exposed to sample the headspace for 30 min. Both the equilibration and sampling times were experimentally determined to obtain an optimal adsorption of the volatiles, and to avoid both under- and over-saturation of the fibre and of the mass spectrometer ion trap. Once sampling was finished, the fibre was withdrawn into the needle and transferred to the injection port of the GC-MS system. Both the sampling and desorption conditions were identical for all the samples. Furthermore, blanks were performed before each first SPME extraction and randomly repeated during each series. Quantitative comparisons of relative peak areas were performed between the same compounds in the different samples.

GC-MS analysis - Gas chromatography–electron impact mass spectrometry (GC–EI-MS) analyses were performed with a Varian CP-3800 gas chromatograph (Varian Inc., Walnut Creek, CA, USA) equipped with an Agilent DB-5 (Agilent Technologies Inc., Santa Clara, CA, USA) capillary column (30 m × 0.25 mm; film thickness 0.25 µm) and a Varian Saturn 2000 ion trap mass detector (Varian Inc., Walnut Creek, CA, USA). Analytical conditions were as follows:

injector and transfer line temperatures, 220 and 240 °C, respectively; oven temperature programmed to rise from 60 to 240 °C, at 3 °C min^{-1}; carrier gas, helium at 1 ml min^{-1}; splitless injection. The identification of constituents was based on a comparison of their retention times with those of authentic samples (when available), comparing their linear retention indices relative to a series of pure *n*-hydrocarbons (C5-C25). Computer matching was also used against commercial (NIST 14 and ADAMS) and laboratory-developed library mass spectra built up from pure substances and components of commercial essential oils of known composition and MS literature data (National Institute of Standards and Technology and NIST, 2014).

Results

Micromorphological investigation

***Trichome morphotypes and distribution pattern* -** Leaves and flowers of *B. acetabulosa* displayed an *indumentum* of non-glandular and glandular trichomes, the latter including both the peltate and capitate types (**Figure 1**).

The peltates were made of a basal cell, a stalk cell, and a large secretory head of 8 cells arranged in a single disc. They were localized on the whole plant epidermis, being scarce on leaves and prevailing on the sepal abaxial surfaces (**Figure 1 a-f**).

Three different types of capitate trichome were found: short-stalked consisting of a basal cell, a stalk cell, and a round 2-4-celled head, mainly located along the veinal system of the whole plant, especially on the leaf and the corolla abaxial sides (**Figure 1 a-c, e**); medium-stalked consisting of a stalk cell, a neck cell, and a 1-2-celled head, occurring on leaf and the calyx abaxial side (**Figure 1 a-c**); and long-stalked, consisting of 2–4 stalk cells, a neck cell, and a globose 2-4-celled secretory head. These hairs were primarily distributed on the leaf adaxial side, on the sepal abaxial side and on the floral peduncle (**Figure 1 b-d, f**).

The observed non-glandular hairs were of two different types: simple, multicellular, uniseriate with distinct articulation between the cells (**Figure 1 a-c, f**), distributed on the surfaces of both the vegetative and the reproductive organs; and stellate multicellular hairs with 4–6 uniseriate arms (**Figure 1 c-e**), distributed on the calyx and the corolla abaxial side.

Histochemistry and ultrastructure - The results of the histochemical investigation on the glandular trichomes are reported in **Table 2** and **Figure 2**.

In the peltate trichomes, all the employed lipophilic tests (**Table 2**, **Figure 2 a**) intensively stained the secreted material, whereas staining reagents such as Alcian Blue and $FeCl_3$ gave negative responses, indicating that the secretion is mainly composed of terpenes. In the secretory cell cytoplasm, the most frequent organelles were multi-shaped electron-dense plastids and a well-developed smooth endoplasmic reticulum (SER) (**Figure 2 b**).

In the short hairs, only the hydrophilic procedures gave faintly positive reactions, indicating the presence of polysaccharidic components (**Table 2**, **Figure 2 c**); $FeCl_3$ test did not stain the secreted material. The secretory cell ultrastructure evidenced Golgi bodies and an abundant rough endoplasmic reticulum (RER) (**Figure 2 d**).

In the medium capitates, the secretion was stained positively both with lipophilic and hydrophilic tests (**Figure 2 e-f**), whereas $FeCl_3$ gave negative results. The trichome ultrastructure showed a dense cytoplasm, numerous small vacuoles, electron-dense plastids, few Golgi bodies, and RER (**Figure 2 g-h**).

In the long capitates, the simultaneous occurrence of lipidic, polysaccharidic, and phenolic compounds was evidenced as indicated by the positive responses to all the employed dyes (**Table 2**, **Figure 2 i-k**). The phenolic fraction was copiously produced, and it was often observed flowing over the glandular head and along the stalk (**Figure 2 k**). At the beginning of the secretion phase, the cytoplasm of the glandular cells showed mitochondria, Golgi bodies, RER cisternae, and plastids with starch granules; in full-active trichomes, Golgi bodies and RER elements became occasional, and plastids lacked starch granules and appeared surrounded by dilated SER cisternae (**Figure 2 l-m**).

Phytochemical investigation

VOCs – The HS-SPME analysis on leaves and flowers of *B. acetabulosa* revealed 46 compounds. In detail, 34 and 21 compounds were identified in the foliar and floral profiles, respectively (**Table 3**).

Almost all the leaf profile was dominated by sesquiterpene hydrocarbons (96.61%), followed by oxygenated sesquiterpenes (2.37%) and non-terpene derivatives (0.12%). The most abundant

compound was γ-muurolene (*31*, 43.63%), followed by β-caryophyllene (*19*, 21.97%). (*E*)-β-Farnesene (*28*, 5.12%), β-bourbonene (*13*, 3.54%), valencene (*33*, 3.19%), *allo*aromadendrene (*29*, 2.53%), α-copaene (*11*, 2.22%), β-copaene (*20*, 2.16%), and carotol (*44*, 2.04%) showed percentages of relative abundance in the range 5.0-2.0%, while β-elemene (*15*, 1.96%), geijerene (*3*, 1.60%), (*E,E*)-α-farnesene (*36*, 1.35%), and *cis*-muurola-4(14),5-diene (*30*, 1.02%) in the range 2.0-1.0%. The remaining compounds occurred in percentages lower than 1.0% or in traces (<0.1%). 25 exclusive compounds were identified, among which valencene (*33*, 3.19%), *allo*aromadendrene (*29*, 2.53%), β-copaene (*20*, 2.16%) and carotol (*44*, 2.04%) were the most abundant. The remaining exclusive compounds accounted for percentages lower than 2.0% or in traces (<0.1%).

Sesquiterpene hydrocarbons represented the main compound class in the floral profile, (45.86%), followed by non-terpene derivatives (21.85%), oxygenated sesquiterpenes (17.14%) and apocarotenoids (11.21%), while the monoterpene class showed only oxygenated compounds (0.99%). γ-Muurolene (*31*, 25.33%) was the dominant compound, followed by (*E*)-nerolidol (*41*, 17.14%), 1-decanal (*5*, 7.51%), β-caryophyllene (*19*, 6.76%), (*E*)-geranyl acetone (*26*, 6.65%) and 1-nonanal (*2*, 5.28%). γ-Elemene (*21*, 3.78%), (*E*)-β-ionone (*32*, 3.27%), aromadendrene (*25*, 3.12%), α-copaene (*11*, 2.65%), β-elemene (*15*, 2.63%), *n*-heptadecane (*46*, 2.34%), *n*-tetradecane (*16*, 2.04%), and *n*-hexadecane (*45*, 2.01%) showed abundances in the range 3.0-2.0%, while *n*-pentadecane (*35*, 1.79%), β-cubebene (*14*, 1.59%), and *cis*-α-ambrinol (*24*, 1.29%) were detected with relative abundances ranging between 2.0 and 1.0%. The other compounds were present with percentages lower than 1.0% or in traces (<0.1%). 12 exclusive compounds were detected, among which (*E*)-nerolidol (*41*, 17.14%) and (*E*)-geranyl acetone (*26*, 6.65%) were the most abundant. The remaining were detected in percentages in the ranges 3.0-2.0%, 2.0-1.0% and <1.0%.

Leaves and flowers shared 9 common compounds: γ-muurolene was prevalent (*31*, 43.63% leaves; 25.33% flowers), followed by β-caryophyllene (*19*, 21.97% leaves; 6.76% flowers), both with a higher percentage in the leaves than in the flowers. (*E*)-β-Farnesene (*28*) and β-bourbonene (*13*) were more abundant in the leaves (5.12%; 3.54%), while in the flowers they were detected only in traces (<0.1%). On the contrary, *n*-decanal (*5*) and *n*-nonanal (*2*)

revealed higher percentages in the flowers (7.51%; 5.28%) than in the leaves (0.12%; traces, <0.1%), while the relative abundances of the compounds (*11*), (*14*), and (*15*) were between 2.0-1.0% and they were quantitatively comparable in the two profiles.

Scientific dissemination

The scientific results reported in the "Micromorphological investigation" and "Phytochemical investigation" sections converged in the realization of a new iconographic apparatus for *B. acetabulosa* at the Ghirardi Botanic Garden (Toscolano Maderno, BS, Italy). In addition to the plant macroscopic features, it highlights the microscopic morphology, the volatile composition of the vegetative and floral *bouquets*, and the noteworthy data on the plant-environment interactions (**Figure 3**).

Discussion

Based on their morphology, the glandular trichomes of *B. acetabulosa* corresponded to the two main types occurring in the Lamiaceae family: peltate and capitate hairs.

The peltate hairs were widespread on the examined vegetative and reproductive organs, being scarce on the leaves and abundant on the sepals; they exhibited an 8-celled head, as already described in *Scutellaria brevibracteata* subsp. *subvelutina* (Rech. f.) Greuter & Burdet (Giuliani *et al.* 2020a). The secreted substances were stained intensively only in response to the lipophilic dyes, especially to the Nadi reagent, indicating that the secretion was exclusively composed of terpenes. Therefore, they were typical essential oil producers, as it occurs in many Lamiaceae (Werker 2000), although in several species of this family chemical complexity of the secretion has also been reported (Giuliani & Maleci Bini 2008). The ultrastructural study on the secretory cells confirmed the histochemical evidence; indeed, the combination of SER and multi-shaped electron-dense plastids with few internal membrane systems is very common for terpenoid producing cells (Hallahan 2000). The collaboration of SER with electron dense plastids can be considered a sign of terpenoid production, even if the role of SER is not yet completely understood (Levine 2004; Giuliani *et al.* 2017). The transfer of terpenoids from one organelle to another and, eventually, to the plasma membrane would be mediated by membrane contact

(Levine 2004). The membrane contacts between electron dense plastids and SER here observed may hence be considered an indication of the activity of terpenoid production.

B. acetabulosa presented three types of capitate hairs, which greatly differed for the overall size, the stalk length, and the shape of the secretory head. The short capitate trichomes were widespread and seemed to be the only type common to all the Lamiaceae species examined so far (Giuliani & Maleci Bini 2008). The hydrophilic procedures only gave faintly positive reactions, indicating the exclusive presence of muco-polysaccharides in the secretion. During the secretory process, the ultrastructure of the head cells evidenced abundant Golgi bodies and the proliferation of RER elements. The development of such compartments may be correlated with the synthesis of polysaccharides (Giuliani & Maleci Bini 2008).

The medium capitates corresponded to the capitate type-II hairs described in several members of the genera *Salvia, Stachys, Sideritis*, and *Scutellaria* (Giuliani & Maleci Bini 2008; Giuliani *et al.* 2020a, 2020b). The secretion resulted heterogeneous, since it was stained positively both with lipophilic and hydrophilic tests. The trichome ultrastructure displayed a dense cytoplasm with numerous small vacuoles, electron-dense plastids, few Golgi bodies, and RER, confirming the histochemical results.

The long capitate hairs were scarce on leaves and numerous on the calyx abaxial side. Noteworthy, these capitate morphotypes were distributed on leaves, whilst, in the other Lamiaceae species examined so far, they were found only on reproductive organs (Giuliani & Maleci Bini 2008). The secreted material was stained positively with all the employed staining procedures, revealing the production and release of a heterogeneous secretion constituted by lipidic, polysaccharidic, and phenolic compounds. Secretory cells ultrastructure supports the histochemical observations; indeed, at the beginning of the secretory phase, the head cells showed mitochondria, Golgi bodies, and well-developed RER elements with plastids owning some starch granules. Plastids are also involved in the production of polyphenol precursors, and the key enzyme for their biosynthesis are localized in the starch granules (Grundhöfer *et al.* 2001). In mature trichomes, Golgi bodies and RER occurred occasionally, while the most striking ultrastructural features were multi-shaped plastids sheathed by periplastidial SER. These ultrastructural features may indicate the initial production of hydrophilic substances and

polyphenols, followed by the release of terpenes in a later stage of the secretory process (Giuliani & Maleci Bini 2008).

The observed glandular trichome morphotypes were consistent with those previously reported for the target-species from Turkey (Yazgan *et al.* 2010), even if a comparison of the distribution pattern was not possible, and from several congeneric species from Egypt (Osman 2012). Regarding to the non-glandular *indumentum,* our observations confirmed the occurrence of the simple uniseriate trichomes on the whole plant epidermis and of the dendritic trichomes, exclusive of the reproductive organs. However, we did not detect the stellate morphotype, previously reported in *B. acetabulosa* (Tutin *et al.* 1972; Yazgan *et al.* 2010) and in other congeneric species (Osman 2012).

Concerning the phytochemical investigation, the foliar profile resulted more complex than the floral one, and this was also evidenced by the presence of a higher number of exclusive compounds, compared to the flowers (25 *vs* 12). Moreover, only 9 common compounds were detected, among which the most abundant were: γ-muurolene, with a relative percentage higher in the leaves than in the flowers (*31*, 43.63% leaves; 25.33% flowers), and β-caryophyllene, the second most abundant compound in the leaves (*19*, 21.97%), while in the flowers it exhibited a lower percentage (*19*, 6.76%). As for the exclusive compounds, valencene (*33*, 3.19%) was the most abundant in the leaves, while in the flowers (*E*)-nerolidol (*41*, 17.14%) prevailed.

On these bases, the comparison with the results of the histochemical survey justifies the terpene productivity, in particular on the petals abaxial surface, where peltate trichomes occurred, and on calyx and floral peduncle, where long-stalked capitates were detected. On the contrary, there is no such marked correspondence for the leaves, where the terpene productivity would appear to be related to the presence of medium-stalked capitates. Due to the absence of works concerning the VOC and essential oil (EO) characterization of the target-species, only a comparison with some congeneric species was possible. Specifically, some studies carried out in Italy investigated the EO composition of *B. hispanica*, *B. nigra* subsp *uncinate* and subsp. *foetida*, *B. undulate*, and *B. saxatilis* (Fraternale *et al.* 2009; Fraternale & Ricci 2014; Riccobono *et al.* 2016; Rigano *et al.* 2017, 2020). Nevertheless, even considering that different analytical methods were adopted, no overlapping exists with the VOC profile of *B. acetabulosa* analysed

herein. The unique phytochemical data that appear to join the species belonging to *Ballota* refer to the tissue compounds, including diterpenes and flavonoids (Morteza-Semnani & Ghanbarimasir 2019; Rosselli *et al.* 2019). All these aspects represent an incentive to deepen the studies on the volatile components at species level.

Concerning the ecological role of the main compounds detected in both the VOC profiles, it emerged that the most abundant one, γ-muurolene (*31*), showed a defensive role, as it was registered for most of the sesquiterpene hydrocarbons (Chizzola 2013; Giuliani *et al*., 2020b). Although it was detected as a common compound, its larger relative abundance in the leaves allowed us to hypothesize a more marked repellent action at the vegetative organs level. Regarding the other common compounds, the attractive-repulsive action of β-caryophyllene (*19*) (Abraham *et al.* 2018; Zhang 2018; Lobo *et al.* 2019; Giuliani *et al.* 2020a, 2020b) is known. Indeed, it attracts honeybees as *Apis cerana* (Abraham *et al.* 2018) and non-pollinators as *Vespa velutina* and species belonging to the genus *Bombus* (Zhang 2018), but it develops a defensive role towards parasites as *Diaphania hyalinata* (Lobo *et al.* 2019), hemiptera and lepidoptera belonging to the genus *Apolygus*, *Aphis* and *Helicoverpa* (Zhang *et al.* 2020). Therefore, in our case study, we may hypothesize that this compound played an attractive role in the flowers and a repulsive action at the leaf level. It should be taken into account that plants have to face two simultaneous conflicting pressures: the need to advertise their pollen as a reward for pollinating insects and the necessity to defend it from predators.

Concerning the leaf exclusive compounds, *allo*aromadendrene (*29*), in synergy with other compounds including β-copaene (*20*), carries out a larvicidal activity towards *Culex quinquefasciatus* (Senthilkumar *et al.* 2008); in addition, in an ecological survey conducted at community level, it was documented that the abundance of this compound would increase in case of interspecific competition (Ormeño *et al.* 2007).

Referring to the floral *bouquet*, the overall abundance of sesquiterpene hydrocarbons makes it difficult to exclude defensive actions even at flower level. To this end, the exclusive compound (*E*)-nerolidol (*41*) represents a powerful signal that stimulates the expression of the plant defences. In fact, its productivity activates a consequential series of cellular and molecular reactions leading the plant to synthetize and accumulate a significant amount of broad-spectrum

379 defensive molecules towards herbivores and different types of parasites (Chen *et al.* 2020).
380 Nerolidol is synthesized in many plants as intermediate of the production of a herbivore-induced
381 terpenoid, DMNT (Chan *et al.* 2016). Moreover, it could develop even an antibacterial action
382 together with β-farnesene (*28*) (Kiryu *et al.* 2018), and nematicide as well (El-Habashy *et al.*
383 2020).
384 In addition, *(E)*-geranyl acetone (*26*) is involved in different VOC-mediated tritrophic interactions
385 (Morawo *et al.* 2016; Pinto-Zevallos *et al.* 2018; Giuliani *et al.* 2020a, 2020b). This suggests
386 potential defensive needs of the target-species against flower parasites. These overall data
387 stimulated our curiosity about investigations on possible parasites known in literature in relation
388 to the species, but information is lacking on these topics.
389 Finally, our study, that originated and takes place at the Ghirardi Botanic Garden, converged
390 towards the fruition of the research products by the general public, following a new approach to
391 the dissemination of scientific data that is increasingly appreciated in literature (Giuliani *et al.*
392 2020, 2020a, 2020b).
393

394 **Conclusion**

395 Our work on *B. acetabulosa* was based on a multidisciplinary study approach. In the
396 micromorphological survey, the occurrence of peltate trichomes and of three capitate
397 morphotypes emerged, each one characterized by a peculiar distribution pattern on the
398 vegetative and the reproductive organs. The application of the histochemical tests was an
399 element of novelty for the target-species; these results were confirmed by the ultrastructural
400 observations, ensuring that the peltates and the long-stalked capitates were the main
401 responsible of the terpenes production, finally resulting in the spontaneous emission of volatiles,
402 characterized through head-space analysis in the phytochemical survey. In the vegetative and
403 floral *bouquets*, the dominance of the sesquiterpene hydrocarbons emerged, among which γ-
404 muurolene, β-caryophyllene and (*E*)-nerolidol were the dominant compounds. Moreover, a
405 comparison with literature data concerning the ecological roles recognized to the most abundant
406 compounds allowed us to hypothesize a prevailing defensive action of the volatile emissions both
407 at the leaf and flower level. These data represented a ”new piece” in the research path aimed at

408 the characterization of the Ghirardi Botanic Garden as a "factory of molecules", an innovative
409 vision placed in an Open Science context.

410

411 **Funding**

412 The authors are grateful to the Lombardy Region for the financial support of the project "Botanic
413 Garden, factory of molecules", under the Call for the Enhancement of Museums Lr. 25/2016,
414 year 2019.

415

416 **Acknowledgments**

417 Our special thanks go to Dr. Patrizia Berera for her contribution in the realization of the labelling.

418

419 **References**

420 Abraham A.A., Verghese A., Muthangi S. (2018) Role of colour and volatile in foraging
421 behaviour of honeybee *Apis cerana* on *Jacquemontia pentanthos*. Journal of Asia-Pacific
422 Entomology **21**:1122–1128.

423 Ascrizzi R., Cioni P.L., Amadei L., Maccioni S., Flamini G. (2017) Geographical patterns of in
424 vivo spontaneously emitted volatile organic compounds in *Salvia* species. Microchemical
425 Journal **133**:13–21.

426 Askun T., Tekwu E.M., Satil F., Modanlioglu S., Aydeniz H. (2013) Preliminary
427 antimycobacterial study on selected Turkish plants (Lamiaceae) against *Mycobacterium*
428 *tuberculosis* and search for some phenolic constituents. BMC Complementary and
429 Alternative Medicine **13**:365.

430 Beccari N., Mazzi V. (1966) *Manuale di tecnica microscopica*. Società Editrice Libraria.

431 Brundrett M.C., Kendrick B., Peterson C.A. (1991) Efficient lipid staining in plant material with
432 Sudan Red 7B or Fluoral Yellow 088 in polyethylene glycol-glycerol. Biotechnic &
433 Histochemistry **66**:111–116.

Chan W.-K., Tan L.T.-H., Chan K.-G., Lee L.-H., Goh B.-H. (2016) Nerolidol: a sesquiterpene alcohol with multi-faceted pharmacological and biological activities. Molecules **21**:529.

Chen S., Zhang L., Cai X., Li X., Bian L., Luo Z., Li Z., Chen Z., Xin Z. (2020) (E)-Nerolidol is a volatile signal that induces defenses against insects and pathogens in tea plants. Horticulture research **7**:1–15.

Chizzola R. (2013) Regular monoterpenes and sesquiterpenes (essential oils). Natural products **10**:973–978.

Couladis M., Tzakou O., Verykokidou E., Harvala C. (2003) Screening of some Greek aromatic plants for antioxidant activity. Phytotherapy Research **17**:194–195.

David R., Carde J.P., David R. (1964) Histochimie–coloration differentielle des inclusions lipidiques et terpeniques des pseudophylles du pin maritime au moyen du reactif NADI. Comptes Rendus Biologies **258**:1338–1340.

Dulger B., Dulger G. (2012) Antimicrobial activity of the leaves of *Ballota acetabulosa* on microorganisms isolated from urinary tract infections. Turkish Journal of Pharmaceutical Sciences **9**:257–262.

Dulger B., Kilcik M.A. (2011a) Antifungal activity of *Ballota acetabulosa* against yeast *Candida* and *Cryptococcus* species. Asian Journal of Chemistry **23**:413–415.

Dulger B., Kilcik M.A. (2011b) Antibacterial activity of *Ballota acetabulosa* against methicillin-resistant *Stapylococcus aureus.* Asian Journal of Chemistry **23**:416–418.

Dumlu M.U., Bulut G.E. (2007) Some biological activity investigations on *Ballota acetabulosa*. Journal of Pharmacy of Istanbul University **39**:53–56.

El-Habashy D.E., Abdel Rasoul M.A., Abdelgaleil S.A.M. (2020) Nematicidal activity of phytochemicals and their potential use for the control of *Meloidogyne javanica* infected eggplant in the greenhouse. European Journal of Plant Pathology **158**:381–390.

Fraternale D., Bucchini A., Giamperi L., Ricci D. (2009) Essential oil composition and antimicrobial activity of *Ballota nigra* L. ssp *foetida*. Natural Product Communications **4**:585–588.

Fraternale D., Ricci D. (2014) Essential oil composition and antifungal activity of aerial parts of

462 *Ballota nigra* ssp *foetida* collected at flowering and fruiting times. Natural Product
463 Communications **9**:1015–1018.
464 Gahan P.B. (1984) *Plant histochemistry and cytochemistry*. Academic Press, London.
465 Giuliani C., Ascrizzi R., Corrà S., Bini L.M., Flamini G., Fico G. (2017) Ultrastructural insight
466 into terpene-producing trichomes and essential oil profile in *Salvia greggii* A. Gray. Flora
467 **236**:107–114.
468 Giuliani C., Bottoni M., Ascrizzi R., Milani F., Flamini G., Fico G. (2020) *Scutellaria caucasica* A.
469 Ham.: Morphological features and headspace characterization. Flora: Morphology,
470 Distribution, Functional Ecology of Plants **269**
471 Giuliani C., Bottoni M., Ascrizzi R., Santagostini L., Papini A., Flamini G., Fico G. (2020a)
472 *Scutellaria brevibracteata* subsp. *subvelutina* (Rech.f.) Greuter & Burdet: morphological
473 and phytochemical characterization. Natural Product Research:1–9.
474 Giuliani C., Bottoni M., Ascrizzi R., Santagostini L., Papini A., Flamini G., Fico G. (2020b) A
475 novel study approach on *Scutellaria altissima* L. cultivated at the Ghirardi Botanic Garden
476 (Lombardy, Italy). Plant Biology **22**:1013–1021.
477 Giuliani C., Maleci Bini L. (2008) Insight into the structure and chemistry of glandular
478 trichomes of Labiatae, with emphasis on subfamily Lamioideae. Plant systematics and
479 evolution **276**:199.
480 Greenspan P., Mayer E.P., Fowler S.D. (1985) Nile red: a selective fluorescent stain for
481 intracellular lipid droplets. The Journal of cell biology **100**:965–973.
482 Grundhöfer P., Niemetz R., Schilling G., Gross G.G. (2001) Biosynthesis and subcellular
483 distribution of hydrolyzable tannins. Phytochemistry **57**:915–927.
484 Hallahan D.L. (2000) Monoterpenoid biosynthesis in glandular trichomes of Labiate plants.
485 Jensen W.A. (1962) *Botanical histochemistry: principles and practice*. San Francisco.
486 Kiryu M., Hamanaka M., Yoshitomi K., Mochizuki S., Akimitsu K., Gomi K. (2018) Rice terpene
487 synthase 18 (OsTPS18) encodes a sesquiterpene synthase that produces an antibacterial
488 (E)-nerolidol against a bacterial pathogen of rice. Journal of General Plant Pathology
489 **84**:221–229.

Levine T. (2004) Short-range intracellular trafficking of small molecules across endoplasmic reticulum junctions. Trends in cell biology **14**:483–490.

Lobo A.P., da Camara C.A.G., de Melo J.P.R., de Moraes M.M. (2019) Chemical composition and repellent activity of essential oils from the leaves of *Cinnamomum zeylanicum* and *Eugenia uniflora* against *Diaphania hyalinata* L.(Lepidoptera: Crambidae). Journal of Plant Diseases and Protection **126**:79–87.

Martínez-Francés V., Rivera D., Heinrich M., Obón C., Ríos S. (2015) An ethnopharmacological and historical analysis of "dictamnus", a European traditional herbal medicine. Journal of Ethnopharmacology **175**:390–406.

El Mokni R., Majdoub S., Jlassi I., Joshi R.K., Hammami S. (2020) Gas chromatography–mass spectrometry profile and antimicrobial activities of *Ballota bullata* Pomel and *B. nigra* L. subsp. *uncinata* (Fiori & Bég.): A comparative analysis. International Journal of Mass Spectrometry **450**

Morawo T., Burrows M., Fadamiro H. (2016) Electroantennogram response of the parasitoid, *Microplitis croceipes* to host-related odors: The discrepancy between relative abundance and level of antennal responses to volatile compound. F1000Research **5**

Morteza-Semnani K., Ghanbarimasir Z. (2019) A review on traditional uses, phytochemistry and pharmacological activities of the genus *Ballota*. Journal of Ethnopharmacology **233**:197–217.

Ormeño E., Bousquet-Mélou A., Mévy J.-P., Greff S., Robles C., Bonin G., Fernandez C. (2007) Effect of intraspecific competition and substrate type on terpene emissions from some Mediterranean plant species. Journal of chemical ecology **33**:277–286.

Osman A.K. (2012) Trichome micromorphology of Egyptian *Ballota* (Lamiaceae) with emphasis on its systematic implication. Pak J Bot **44**:33–46.

Pinto-Zevallos D.M., Bezerra R.H.S., Souza S.R., Ambrogi B.G. (2018) Species-and density-dependent induction of volatile organic compounds by three mite species in cassava and their role in the attraction of a natural enemy. Experimental and Applied Acarology **74**:261–274.

Psaras G.K. (1986) Chloroplast Arrangement along Intercellular Spaces in the Leaves of a Mediterranean Subshrub. Journal of Plant Physiology **126**:189–193.

Psaras G.K., Rhizopoulou S. (1995) Mesophyll structure during leaf development in *Ballota acetabulosa*. New Phytologist **131**:303–309.

Riccobono L., Ben Jemia M., Senatore F., Bruno M. (2016) Chemical composition and biological activity of the essential oil of *Ballota hispanica* (L.) Benth. growing wild in Sicily. Plant Biosystems **150**:1065–1071.

Rigano D., Formisano C., Rosselli S., Badalamenti N., Bruno M. (2020) GC and GC-–MS analysis of volatile compounds from *Ballota nigra* subsp. *uncinata* collected in Aeolian islands, Sicily (Southern Italy). Natural Product Communications **15**:1–7.

Rigano D., Marrelli M., Formisano C., Menichini F., Senatore F., Bruno M., Conforti F. (2017) Phytochemical profile of three *Ballota* species essential oils and evaluation of the effects on human cancer cells. Natural Product Research **31**:436–444.

Rosselli S., Fontana G., Bruno M. (2019) A Review of the Phytochemistry, Traditional Uses, and Biological Activities of the Genus *Ballota* and *Otostegia*. Planta Medica **85**:869–910.

Sahpaz S., Skaltsounis A.-L., Bailleul F. (2002) Polyphenols from *Ballota acetabulosa*. Biochemical Systematics and Ecology **30**:601–604.

Senthilkumar A., Kannathasan K., Venkatesalu V. (2008) Chemical constituents and larvicidal property of the essential oil of *Blumea mollis* (D. Don) Merr. against *Culex quinquefasciatus.* Parasitology research **103**:959–962.

Tutin T., Heywood V., Burges N., Moore D., Valentine D., Waters S., Webbs D. (1972) *Flora Europea 3*. Cambridge University Press, Cambridge UK.

Werker E.B.T.-A. in B.R. (2000) Trichome diversity and development. In: Academic Press, pp 1–35.

Yazgan A.N., Yilmaz G., Sever Yilmaz B. (2010) Anatomical studies on *Ballota acetabulosa* (L.) Benth. Ankara Universitesi Eczacilik Fakultesi Dergisi **39**:265–274.

Yilmaz B.S., Çitoğlu G.S. (2003) High Performance Liquid Chromatographic Analysis of some Diterpenoids of the *Ballota* species. Fabad Journal of Pharmaceutical Sciences **28**:13–17.

Zhang X. (2018) Floral volatile sesquiterpenes of *Elsholtzia rugulosa* (Lamiaceae) selectively attract Asian honey bees. Journal of Applied Entomology **142**:359–362.

Zhang L., Lu G., Huang X., Guo H., Su X., Han L., Zhang Y., Qi Z., Xiao Y., Cheng H. (2020) Overexpression of the caryophyllene synthase gene GhTPS1 in cotton negatively affects multiple pests while attracting parasitoids. Pest Management Science **76**:1722–1730.

572 **Figure Legend**

573 **Figure 1.** SEM micrographs showing trichome morphotypes and distribution pattern in *Ballota*
574 *acetabulosa* (L.) Benth. **(a)** Leaf abaxial surface with abundant short capitates, occasional
575 medium capitates and dendritic non-glandular trichomes. **(b)** Leaf adaxial surface with short
576 capitates, occasional medium and long capitates and simple non-glandular trichomes. **(c-d)**
577 Calyx abaxial surface: general view **(c)** and detail **(d)** with abundant peltates and the three
578 morphotypes of capitates; notice the abundance of the dendritic trichomes. **(e)** Corolla abaxial
579 surface at the apical region with peltates, short capitates and dendritic non-glandular trichomes.
580 **(f)** Floral pedicel with short capitates, long capitates and simple non-glandular trichomes.

581

582 **Figure 2. (a)** Histochemistry of the peltate trichome: Nadi reagent, LM. **(b)** Ultrastructure of
583 the peltate trichome, TEM. **(c)** Histochemistry of the short-stalked capitate trichome: Nadi
584 reagent, LM. **(d)** Ultrastructure of the short-stalked capitate trichome, TEM. **(e, f)**
585 Histochemistry of the medium-stalked capitate trichome: Nadi reagent **(e)**, Ruthenium Red **(f)**,
586 LM. **(g, h)** Ultrastructure of the medium-stalked capitate trichome, TEM. **(i-k)** Histochemistry
587 of the long-stalked capitate trichome: Nile Red **(i)**, Nadi reagent **(j)**, $FeCl_3$ **(k)**, LM. **(l, m)**
588 Ultrastructure of the long-stalked capitate trichome at the beginning (l) and at the end (m) of
589 the secretory process, TEM.

590 *Scale bars*: a, c, e-f, i-k, 25 µm; b, d, g-h, l-m, 1 µm.

591 *Symbols*: cw, cell wall; g, Golgi bodies; N, nucleus; p, plastid; rer, RER; ss, subcuticular space;
592 ser, SER; v, vacuols.

593

594 **Figure 3.** New labelling of *Ballota acetabulosa* (L.) Benth. at the Ghirardi Botanic Garden.

Table 1. Distribution pattern of the glandular and non-glandular trichomes in *Ballota acetabulosa* (L.) Benth.

Trichome type	Leaf		Calyx		Corolla		Floral peduncle
	adax	abax	adax	abax	adax	abax	
peltate	±	±	-	±	-	++	±
short capitate	+	++	+	+	+	++	+
medium capitate	+	±	-	±	-	-	±
long capitate	±	-	-	+	-	-	+
simple non-glandular	++	-	-	±	+	+	+
dendritic non-glandular	-	+	-	+	-	+	-

Symbols: (-) missing, (±) sporadic, (+) present, (++) abundant

Table 2. Results of the histochemical tests on the glandular trichomes of *Ballota acetabulosa* (L.) Benth.

Stainings	Target-compounds	peltate	short capitate	medium capitate	long capitate
Fluoral Yellow-088	Total lipids	+	–	±	+
Nile Red	Neutral lipids	+	–	±	+
Nadi reagent	Terpenoids	++	–	±	+
Ruthenium Red	Acid polysaccharides	–	+	+	+
Alcian Blue	Muco-polysaccharides	–	±	+	+
Ferric Trichloride	Polyphenols	–	–	–	+

Symbols: (–) negative response; (+) positive response; (++) intensely positive response

Table 3. HS-SPME profiles of the leaves and flowers of *Ballota acetabulosa* (L.) Benth.

	I.r.i.	Compounds	Relative Abundance (%)	
			Leaves	Flowers
1	1034	1,8-cineole	tr	-
2	1102	1-nonanal	tr	5.28
3	1143	geijerene	1.6	-
4	1199	*n*-dodecane	tr	-
5	1204	1-decanal	0.12	7.51
6	1241	methyl carvacrol	-	0.99
7	1292	1-tridecene	tr	-
8	1340	δ-elemene	0.19	-
9	1351	α-cubebene	0.32	-
10	1368	cyclosativene	tr	-
11	1376	α-copaene	2.22	2.65
12	1380	daucene	0.69	-
13	1384	β-bourbonene	3.54	tr
14	1390	β-cubebene	0.96	1.59
15	1392	β-elemene	1.96	2.63
16	1399	*n*-tetradecane	-	2.04
17	1410	α-gurjunene	0.26	-
18	1415	1,7-*di*-*epi*-β-cedrene	0.18	-
19	1420	β-caryophyllene	21.97	6.76
20	1429	β-copaene	2.16	-
21	1433	γ-elemene	-	3.78
22	1438	*trans*-α-bergamotene	0.85	-
23	1439	α-guaiene	0.82	-
24	1440	*cis*-α-ambrinol	-	1.29
25	1441	aromadendrene	-	3.12
26	1453	(*E*)-geranyl acetone	-	6.65
27	1454	α-*neo*-clovene	0.12	-
28	1460	(*E*)-β-farnesene	5.12	tr
29	1461	*allo*aromadendrene	2.53	-
30	1462	*cis*-muurola-4(14),5-diene	1.02	-
31	1477	γ-muurolene	43.63	25.33
32	1490	(*E*)-β-ionone	-	3.27
33	1492	valencene	3.19	-
34	1498	α-muurolene	0.36	-
35	1500	*n*-pentadecane	-	1.79
36	1507	(*E,E*)-α-farnesene	1.35	-
37	1513	*trans*-γ-cadinene	0.47	-
38	1524	δ-cadinene	0.98	-
39	1529	lilial	-	0.88
40	1538	α-cadinene	0.12	-
41	1565	(*E*)-nerolidol	-	17.14
42	1575	germacrene D-4-ol	0.12	-
43	1581	caryophyllene oxide	0.21	-
44	1594	carotol	2.04	-
45	1600	*n*-hexadecane	-	2.01
46	1700	*n*-heptadecane	-	2.34
		Oxygenated monoterpenes	**-**	**0.99**
		Sesquiterpene hydrocarbons	**96.61**	**45.86**
		Oxygenated Sesquiterpenes	**2.37**	**17.14**
		Apocarotenoids	**-**	**11.21**
		Non-terpene derivatives	**0.12**	**21.85**
		Total	**99.10%**	**97.05%**

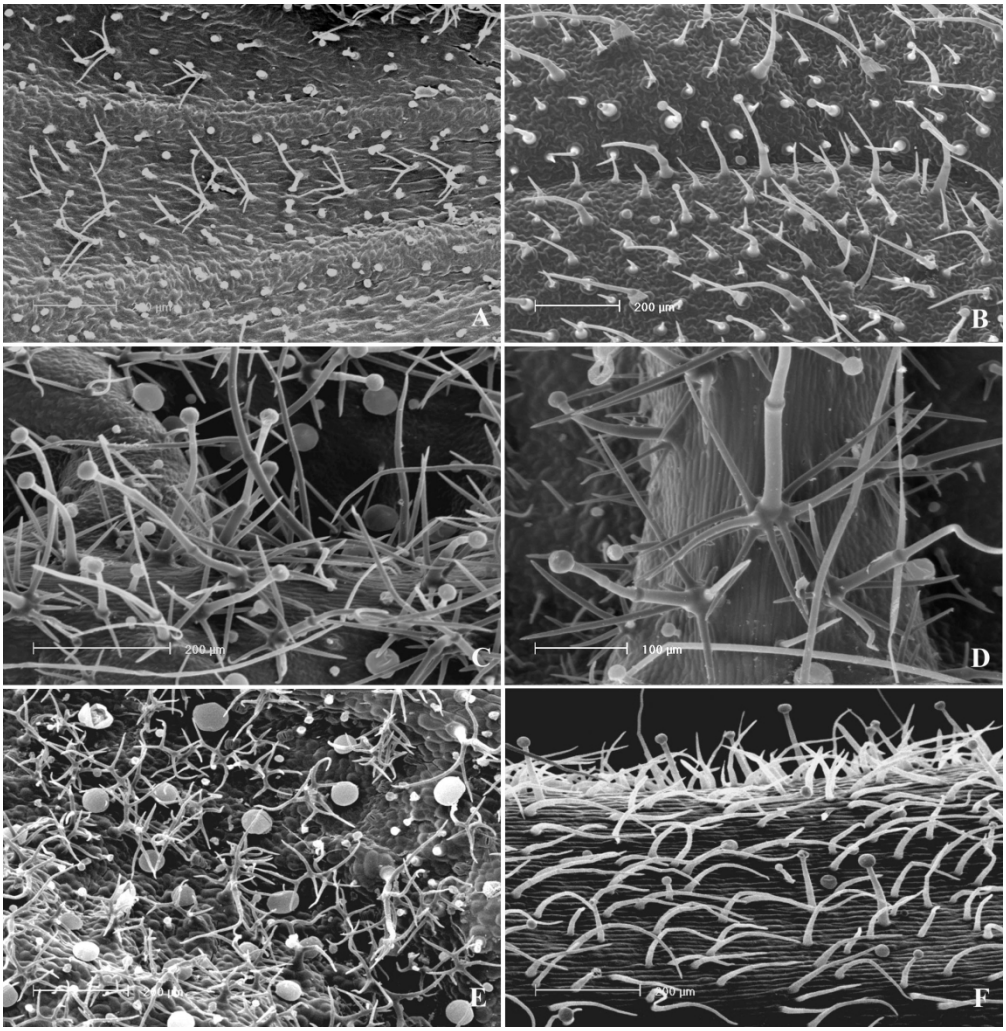

177x181mm (300 x 300 DPI)

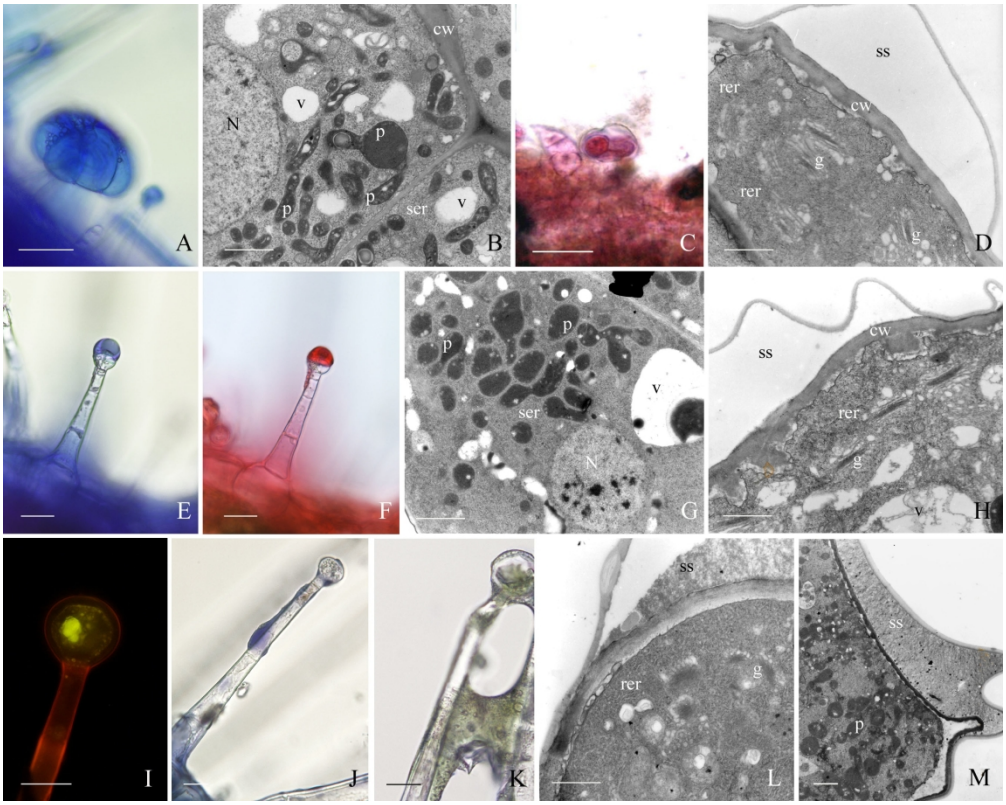

228x182mm (300 x 300 DPI)

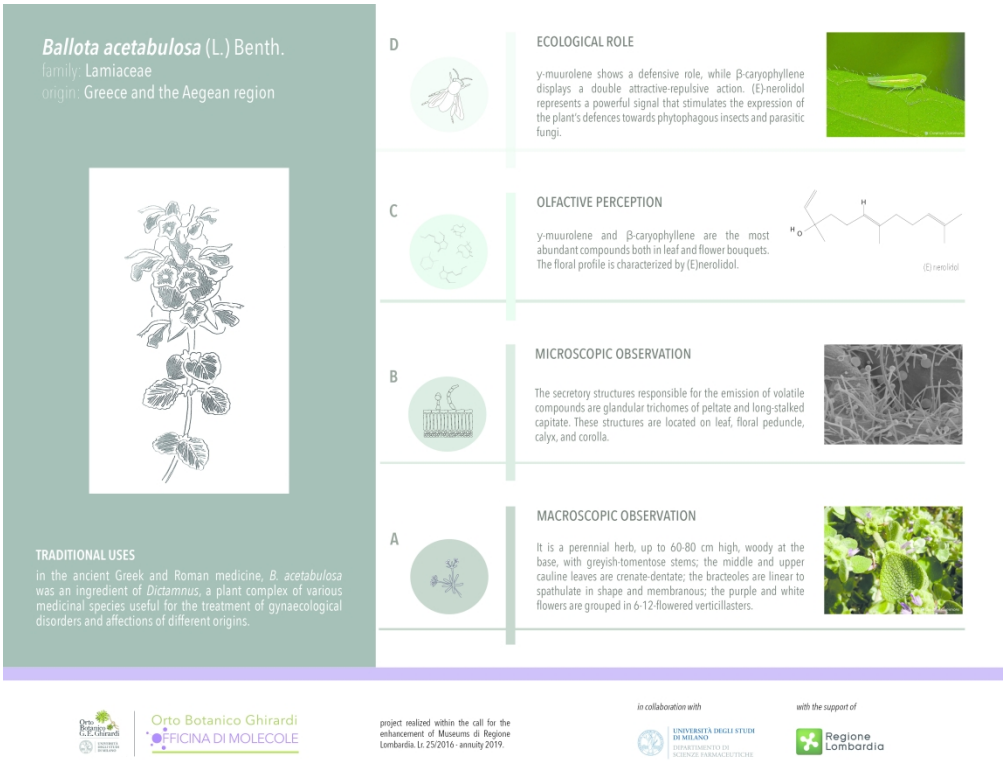

350x270mm (300 x 300 DPI)